REPORT SD-TR-89-46

(4)

Coupled Multiline CW HF Lasers: Experimental Performance

J. M. BERNARD, R. A. CHODZKO, and H. MIRELS
Aerophysics Laboratory
Laboratory Operations
The Aerospace Corporation
El Segundo, CA 90245

1 July 1989

Prepared for

SPACE SYSTEMS DIVISION
AIR FORCE SYSTEMS COMMAND
Los Angeles Air Force Base
P.O. Box 92960
Los Angeles, CA 90009-2960

This report was submitted by The Aerospace Corporation, El Segundo, CA 90245, under Contract No. F04701-85-C-0086-P00016 with the Space Systems Division, P.O. Box 92960, Los Angeles, CA 90009-2960. It was reviewed and approved for The Aerospace Corporation by W. P. Thompson, Director, Aerophysics Laboratory. Capt Scott W. Levinson was the project officer.

This report has been reviewed by the Public Affairs Office (PAS) and is releasable to the National Technical Information Service (NTIS). At NTIS, it will be available to the general public, including foreign nationals.

This technical report has been reviewed and is approved for publication. Publication of this report does not constitute Air Force approval of the report's findings or conclusions. It is published only for the exchange and stimulation of ideas.

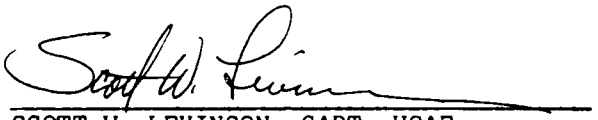

SCOTT W. LEVINSON, CAPT, USAF
Project Officer
SSD/CNID

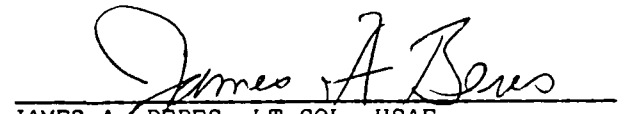

JAMES A. BERES, LT COL, USAF
Director, AFSTC/WCO OL-AB

UNCLASSIFIED

SECURITY CLASSIFICATION OF THIS PAGE

REPORT DOCUMENTATION PAGE

1a. REPORT SECURITY CLASSIFICATION Unclassified	1b. RESTRICTIVE MARKINGS
2a. SECURITY CLASSIFICATION AUTHORITY	3. DISTRIBUTION/AVAILABILITY OF REPORT Approved for public release; distribution unlimited.
2b. DECLASSIFICATION/DOWNGRADING SCHEDULE	
4. PERFORMING ORGANIZATION REPORT NUMBER(S) TR-0086A(2060)-2	5. MONITORING ORGANIZATION REPORT NUMBER(S) SD-TR-89-46
6a. NAME OF PERFORMING ORGANIZATION The Aerospace Corporation Laboratory Operations 6b. OFFICE SYMBOL (If applicable)	7a. NAME OF MONITORING ORGANIZATION Space Systems Division
6c. ADDRESS (City, State, and ZIP Code) El Segundo, CA 90245	7b. ADDRESS (City, State, and ZIP Code) Los Angeles Air Force Base Los Angeles, CA 90009-2960
8a. NAME OF FUNDING/SPONSORING ORGANIZATION 8b. OFFICE SYMBOL (If applicable)	9. PROCUREMENT INSTRUMENT IDENTIFICATION NUMBER F04701-85-C-0086-P00016
8c. ADDRESS (City, State, and ZIP Code)	10. SOURCE OF FUNDING NUMBERS PROGRAM ELEMENT NO. / PROJECT NO. / TASK NO. / WORK UNIT ACCESSION NO.

11. TITLE (Include Security Classification)

Coupled Multiline CW HF Lasers: Experimental Performance

12. PERSONAL AUTHOR(S)

Bernard, Jay M.; Chodzko, Richard A.; and Mirels, Harold

13a. TYPE OF REPORT	13b. TIME COVERED	14. DATE OF REPORT (Year, Month, Day)	15. PAGE COUNT
	FROM _____ TO _____	1 July 1989	23

16. SUPPLEMENTARY NOTATION

17. COSATI CODES			18. SUBJECT TERMS (Continue on reverse if necessary and identify by block number)
FIELD	GROUP	SUB-GROUP	Laser resonators Lasers Phased array

19. ABSTRACT (Continue on reverse if necessary and identify by block number)

The experimental performance of two coupled arc-driven continuous wave HF chemical lasers employing unstable resonators has been measured. Mode-matched adjoint coupling of 20% was accomplished with a beamsplitter. Multiline interference fringes were obtained when the two laser output beams were overlapped in the near field. The mutual coherence of the two beams was inferred from measurement of the visibility of these fringes. Single line fringe visibility was measured as 98% +/- 2% for each of the two strongest lines. These data suggest that the two outputs are nearly completely phase-locked. This locking was found to be insensitive to perturbations in the lengths of the laser resonators. Mode-beating measurements also suggest complete phase locking, as the coupled system behaves like a single laser cavity. The coherent combination of the two laser output beams was attempted by minimizing the optical path difference between these beams, at an external measuring station. This was achieved by changing the external path length of one beam until maximum multiline visibility (97%) was obtained. Demonstration of the corresponding far-field peak intensity enhancement and reduction in spot size for the combined outputs was also accomplished.

20. DISTRIBUTION/AVAILABILITY OF ABSTRACT	21. ABSTRACT SECURITY CLASSIFICATION
☐ UNCLASSIFIED/UNLIMITED ☒ SAME AS RPT. ☐ DTIC USERS	Unclassified
22a. NAME OF RESPONSIBLE INDIVIDUAL	22b. TELEPHONE (Include Area Code) / 22c. OFFICE SYMBOL

DD FORM 1473, 84 MAR

83 APR edition may be used until exhausted.
All other editions are obsolete

SECURITY CLASSIFICATION OF THIS PAGE

UNCLASSIFIED

PREFACE

The authors are indebted to H. A. Bixler and T. J. Bixler for the maintenance and operation of the arc-driven chemical laser facility and for their patience and expertise in the tedious alignment procedure.

CONTENTS

FIGURES

I. INTRODUCTION

Phased arrays of laser beams provide a means to increase the power and aperture size of laser transmitters. The larger aperture is synthesized by combining the outputs of several phase-locked smaller laser systems. Coupling of lasers is one approach to achieve the required phasing of the multiple outputs. In coupled devices, part of the output of one laser is injected into a second laser in order to achieve phase-locking between the two outputs. This process is repeated for all of the lasers in the coupled system. For the purpose of this report, we define coupling as the process of injection of part of one output into a second laser. Phase-locking is defined as the achievement of complete mutual coherence between the two outputs for every spectral line. Phase-matching is defined as the coherent combination (i.e., achievement of zero phase difference for all lines) of the two beams at the diagnostic location.

A theoretical investigation of coupled resonators was reported in 1972 by Spencer and Lamb.[1] In their one-dimensional model, coupling was accomplished through a "dielectric bump" with $\pi/2$ phase shift. This theory was extended to arbitrary phase shift by Mirels,[2] who also investigated the effect of gain saturation on these results.[3] All of these single-line theories predict that phase-locking is sensitive to the coupling fraction and to changes in resonator length on the order of a quarter-wavelength. Palma and Fader[4] have experimentally verified these results using coupled single-line CO_2 lasers. They found that the locking range (the distance range over which phase-locking occurs) increased from a tenth-wavelength to a quarter-wavelength as the coupling fraction was increased from 9% to 50%.

The present experimental study investigates the coupling of multiline, multimode, inhomogenously broadened HF chemical lasers. The theoretical single-line results suggest[2] that if the resonator lengths are within the locking range for one line of a multiline laser, the other lines may or may not be within their locking ranges. This could result in about half of the output lines being phase-locked. Mirels[2] has suggested that mode competition

may quench the unstable modes of the coupled system, in which case every output mode of the system would be phase-locked, without length sensitivity or power decrement.

We have previously reported[5] results of preliminary experiments on two strongly coupled multiline CW HF chemical lasers employing confocal unstable resonators. From measurements of the visibility of fringes obtained by overlapping the two output beams in the near-field, we concluded that the multiline outputs were completely phase-locked with no sensitivity to resonator length. The visibility of single line components of the multiline interference pattern was 0.98, confirming that each line was phase-locked. Measured multiline visibilities were not as high, since the path lengths for the two beams were not equalized. In this report, we give further measurements on this strongly coupled system, which verify the above conclusions. First, the near-field fringe scans are shown, and the maximum multiline visibility is measured by equalizing the optical path lengths for the two beams. Further evidence of complete phase-locking is provided by measurements of the characteristic longitudinal mode-beat frequencies for the independent and coupled lasers. Finally, the narrowing and peak intensity enhancement of the far-field focused spot for the coupled outputs is measured. These experiments were conducted on an electric-arc driven supersonic-diffusion CW HF chemical laser.[6]

II. EXPERIMENTAL APPARATUS

A schematic diagram of the coupled resonator configuration is shown in Fig. 1. Mirrors M_1 and M_2, and M_3 and M_4, comprise two nominally identical confocal unstable resonators of length 1.5 m, magnification 1.4, and equivalent Fresnel number 4.1 (based on the average wavelength of 2.8 μm and the scraper hole diameter of 7.1 mm). The resonator paths are arranged to use two separate portions of the HF gain medium. The arc-driven, supersonic diffusion HF gain generator is described in Ref. 6. The two laser outputs emerge from hole-scraper mirrors M_5 and M_6, and a portion of each output is directed into the other resonator through coupling beamsplitter CB. One side of CB is a 20% transmission (80% reflection) coating, and the other side is antireflection coated. The reflected component of each beam is routed to mirrors M_7 and M_8, which become the phased array output aperture for the coupled laser system. CP is a ZnSe compensating plate in the path of one beam to provide the same dispersion encountered by the other beam, which traveled through the coupling beamsplitter before being reflected. Mirrors M_9 and M_{10} are mounted together on a motorized translation stage so that the optical path length traversed by one beam can be adjusted relative to the other. The alignment of the beam as it leaves M_{10} is not affected by the path length adjustment, so the translating combination of M_9 and M_{10} is termed an "optical trombone."

The diagnostic apparatus used to characterize the two output beams included total power, beam quality, spectral line content, near-field fringe visibility, mode-beating radio frequency (RF) spectral content, and scans of the far-field spot size. The near-field fringe scans and the far-field intensity scans were made using a rotating mirror to translate the intensity pattern over a pinhole, behind which was a Judson model LD12 indium-arsenide room temperature detector. Single-line components of the multiline pattern were obtained by inserting spectral line filters in front of the pinhole. These data were recorded on magnetic disk using a Norland 3001 digital oscilloscope. Two intracavity shutters and two external shutters facilitated

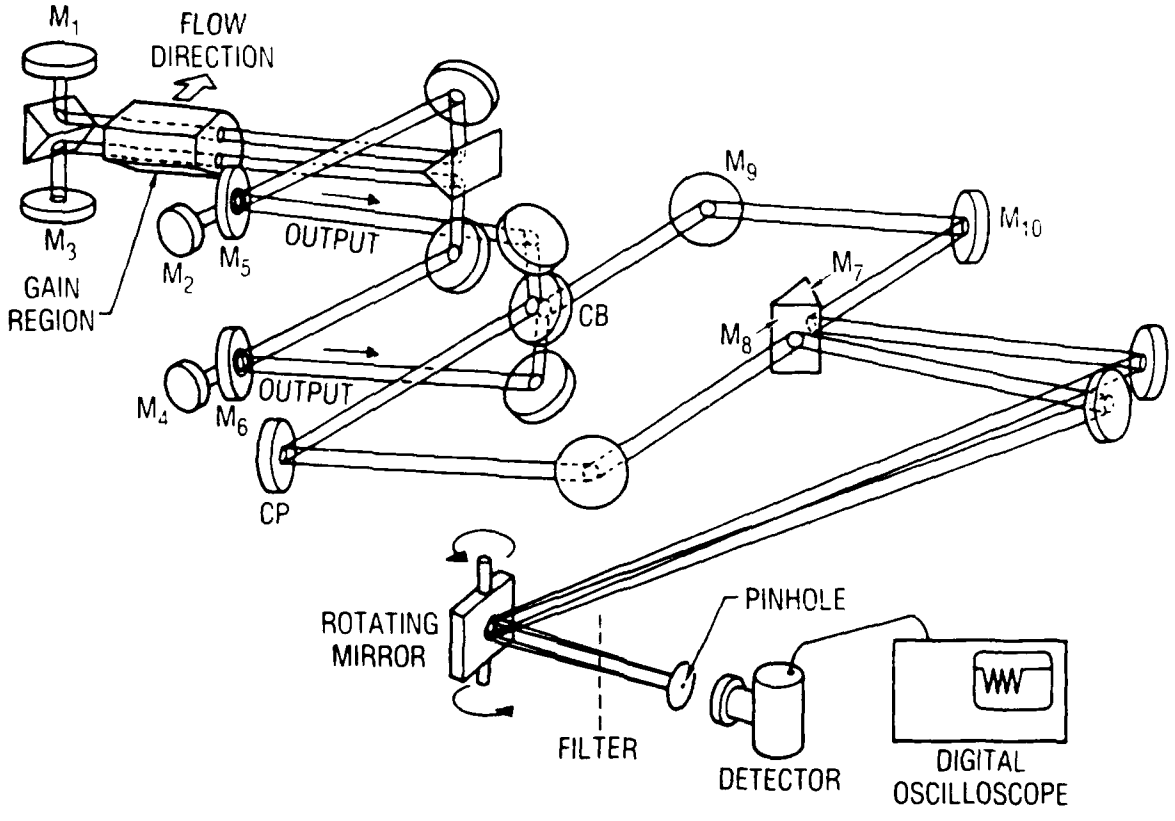

Fig. 1. Schematic Diagram of the Coupled Unstable Resonator Experiment

comparison of the results for coupled and uncoupled operation of the individual lasers and for individual and combined outputs for the coupled system.

The beam quality was evaluated by measurement of the power transmitted through an aperture whose diameter equals that of the first null in the theoretical far-field pattern. The beam quality parameter n^2 is the ratio of theoretically predicted to experimentally measured power transmitted through the aperture. The theoretical values of the aperture diameter and percent power transmitted are based on a geometric optics estimate for the near-field geometry and an assumption of uniform near-field phase and intensity.

III. EXPERIMENTAL RESULTS

The individual, uncoupled beams were first characterized, displaying nearly diffraction-limited beam quality ($n^2 = 1.02$). The laser line spectrum was the same, whether coupled or not, with most of the power appearing on $P_2(6)$ (comprising 36% of the output power) and $P_2(7)$ (29%). The remainder of the power appeared on $P_2(5)$ (14%), $P_1(5)$ (12%), $P_2(8)$ (3%), $P_1(7)$ (2%), $P_2(4)$ (1.5%), $P_1(9)$ (1%), and $P_2(3)$ (0.5%). The laser output power was 50 W per laser when uncoupled and 75 W per laser when coupled. The power increase upon injecting 20% of one output into the other resonator indicates that the gain was not saturated by the intracavity radiation.

A. INTERFERENCE FRINGE VISIBILITY

Interference fringes were observed when the two output beams were overlapped in the near field. Figure 2 is a photograph of the thermal image of these fringes, and Fig. 3 shows one-dimensional centerline scans of these fringes. Figure 3a is the single-line $P_2(6)$ component of the multiline pattern, and Fig. 3b is the multiline fringe pattern.

The visibility measured from these traces is

$$V_{measured} = (v_{max} - v_{min})/(v_{max} + v_{min})$$

where v_{max} and v_{min} are the maximum and minimum detector voltages measured from the zero-intensity baseline of the oscilloscope trace, respectively. The actual fringe visibility is

$$V_{actual} = (I_{max} - I_{min})/(I_{max} + I_{min})$$

where I_{max} and I_{min} are the maximum and minimum intensities in the fringe pattern. The finite size of the pinhole in front of the detector results in a maximum (or minimum) voltage that is not representative of I_{max} (or I_{min}) but is spatial average of the intensity in the region near I_{max} (or I_{min}). We have calculated the effect of this averaging for fringes with a cosine-wave

Fig. 2. Thermal Image of the Multiline Near-Field Fringe Pattern

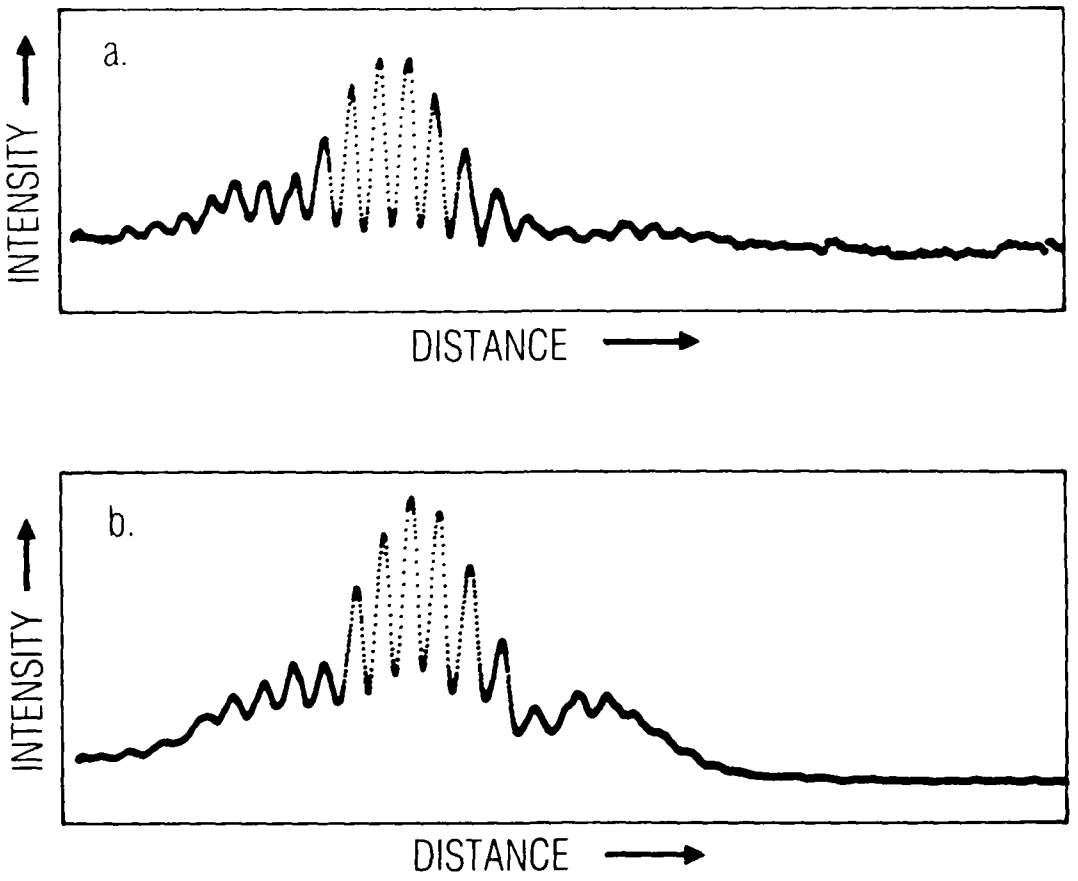

Fig. 3. (a) Centerline Scan of the $P_2(6)$ Component of the Multiline Near-Field Interference Fringes; (b) Centerline Scan of the Multiline Near-Field Fringes.

intensity distribution and find that $V_{measured} = 0.92\ V_{actual}$ for the pinhole diameter (125 μm) and fringe spacing (500 μm) encountered in our experiments. The multiline interference fringe visibility is further degraded by a factor of 0.95 because of a small (150 μm) difference in thickness between the coupling beamsplitter and the compensating plate. This distance mismatch results in incomplete compensation for the different phase shifts encountered by different spectral lines for the beam that goes through the coupling beamsplitter with respect to the beam that goes through the compensating plate. This calculation was made using the spectral power distribution quoted earlier and the known dispersion of the ZnSe plates. The relations between the measured and actual visibilities are thus

$$V_{single\text{-}line} = V_{measured}/0.92$$
$$V_{multiline} = (V_{measured}/0.92)/0.95$$

For Fig. 3a, $V_{single\text{-}line}$ is 0.98, indicating nearly complete phase locking of that single line component. An identical result was obtained for $P_2(5)$, suggesting that since these lines were chosen at random, all of the lines were probably phase-locked. The multiline scan shown in Fig. 3b, for which $V_{multiline} = 0.88$, was taken without equalizing the optical path lengths for the two beams from the cavity concave mirrors to the diagnostic overlap region. The resulting phase mismatch accounts for the departure of $V_{multiline}$ from a value near one. We verified this by stopping the rotating mirror to fix the fringe pattern in front of the pinhole and by translating the optical trombone to generate the fringe minima and maxima as a function of optical path difference (OPD) between the two beams. The measured fringe pattern vs. OPD is shown in Fig. 4, for which the phase-matched central fringe is indicated by an arrow. The corrected visibility of this fringe is $V_{multiline} = 0.97$, indicating nearly ideal phase matching of the multiline output. This result was obtained at several values of the resonator lengths.

B. MODE BEATING

Measurement of the difference frequencies in the laser longitudinal mode spectrum is accomplished by allowing the optical spectrum of a single spectral

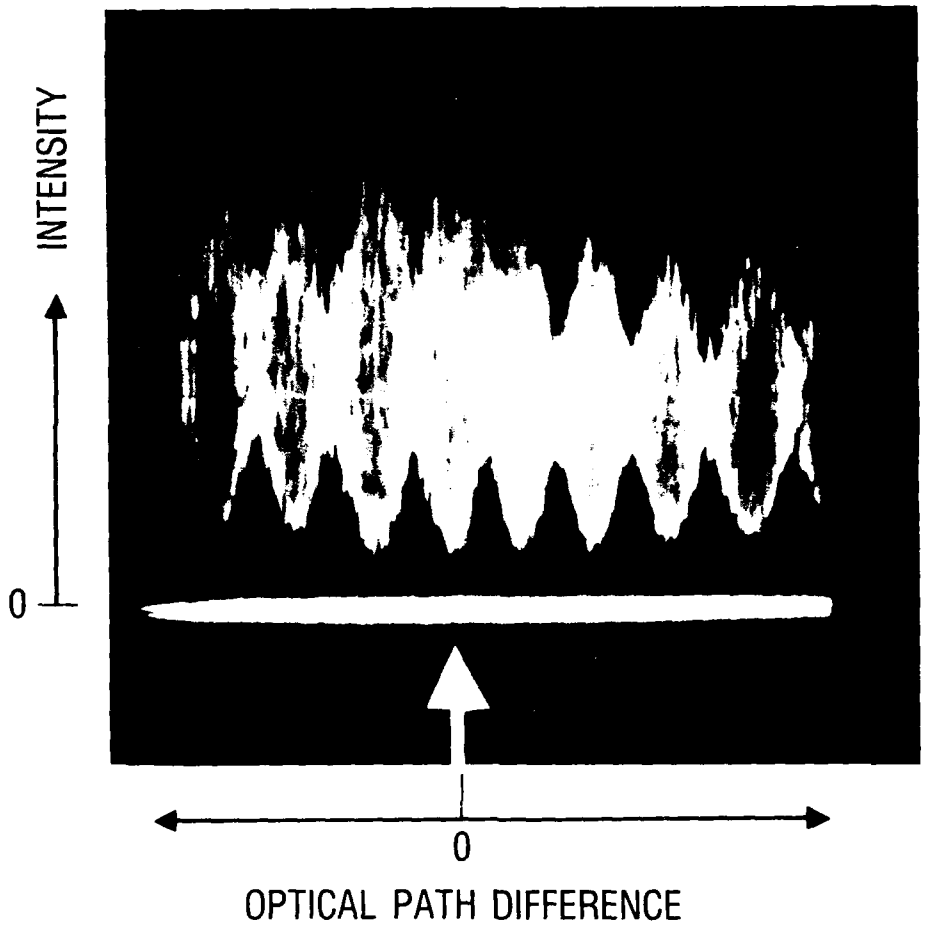

Fig. 4. Multiline Fringe Intensity as a Function of Optical Path Difference between the Two Output Beams

line [e.g., $P_2(6)$] to beat with itself at the detector surface. The longitudinal modes resonant with a laser cavity of length L are separated in frequency by c/2L, so that if two longitudinal modes are output by the given transition, the power spectrum of the detector current will have a strong component at c/2L. A representative mode-beating measurement of the detector power spectrum is shown in Fig. 5 for one of the individual uncoupled lasers. L for the individual lasers is the distance between M_1 and M_2 (or M_3 and M_4) and is nominally 1.5 m. In addition to typical low-frequency beats (presumably the transverse mode spectrum), a strong component is seen near 100 MHz, precisely c/2L for a resonator 1.5 m in length. The spectrum taken for a coupled laser is shown in Fig. 6. A small component is occasionally seen at 100 MHz, but the predominant beat is at 40 MHz, implying a characteristic length of 3.4 m, which is approximately the sum of the two resonator lengths plus the coupling path length (2L plus the distance traveled through the coupling beamsplitter between M_5 and M_6). Apparently, longitudinal modes are created that are resonant with the length of the coupled system rather than the length of the individual resonators. This suggests that the coupled system behaves as a single laser device with two outputs. The two outputs for such a system are completely phase-locked, as they are resonant modes of a single device. Thus the mode-beating results are independent evidence that the two outputs are completely phase-locked. Again, no sensitivity to the resonator lengths was found.

C. FAR-FIELD INTENSITY DISTRIBUTION

Finally, a far-field measurement was made to demonstrate the narrowing and peak intensity enhancement expected when two phase-matched beams are focused to a common spot. The theoretical far-field centerline scan of the focused spot for two phase-matched and two independently operating lasers is shown in Fig. 7. These calculations are based in uniform phase and intensity beams whose near-field apertures are also shown in Fig. 7. This scan is made in the horizontal plane, as the near-field apertures are beside each other. As this figure shows, the spot corresponding to phase-matched lasers is approximately three times narrower than the spot corresponding to two independent lasers. Figure 8a shows a single line [$P_2(6)$] scan of the

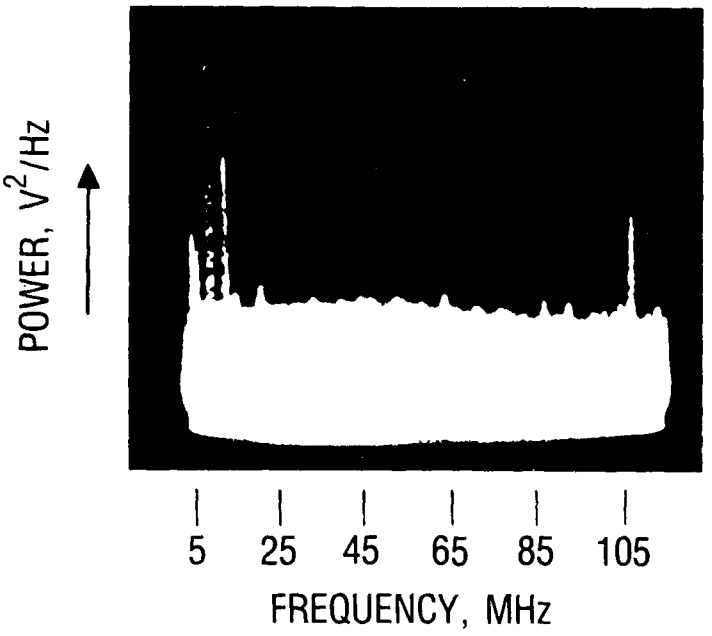

Fig. 5. Longitudinal Mode-Beat Spectrum for an Individual Uncoupled Laser

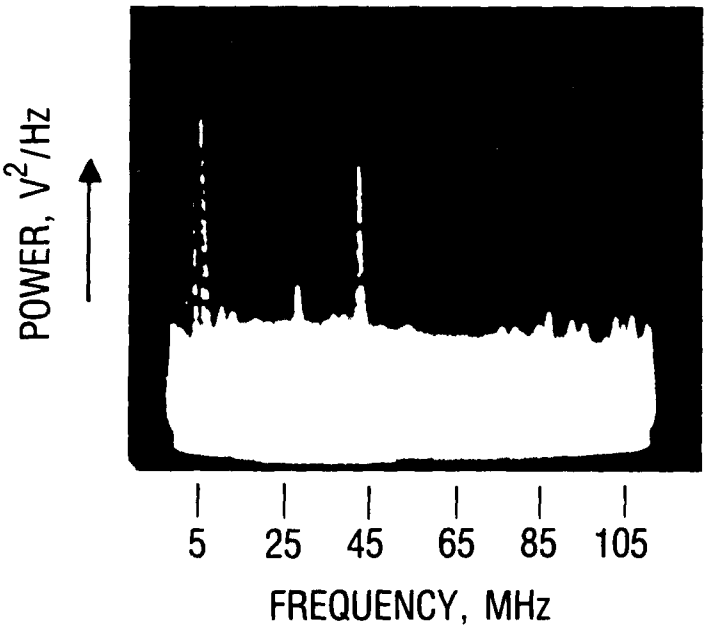

Fig. 6. Longitudinal Mode-Beat Spectrum for an Individual Coupled Laser

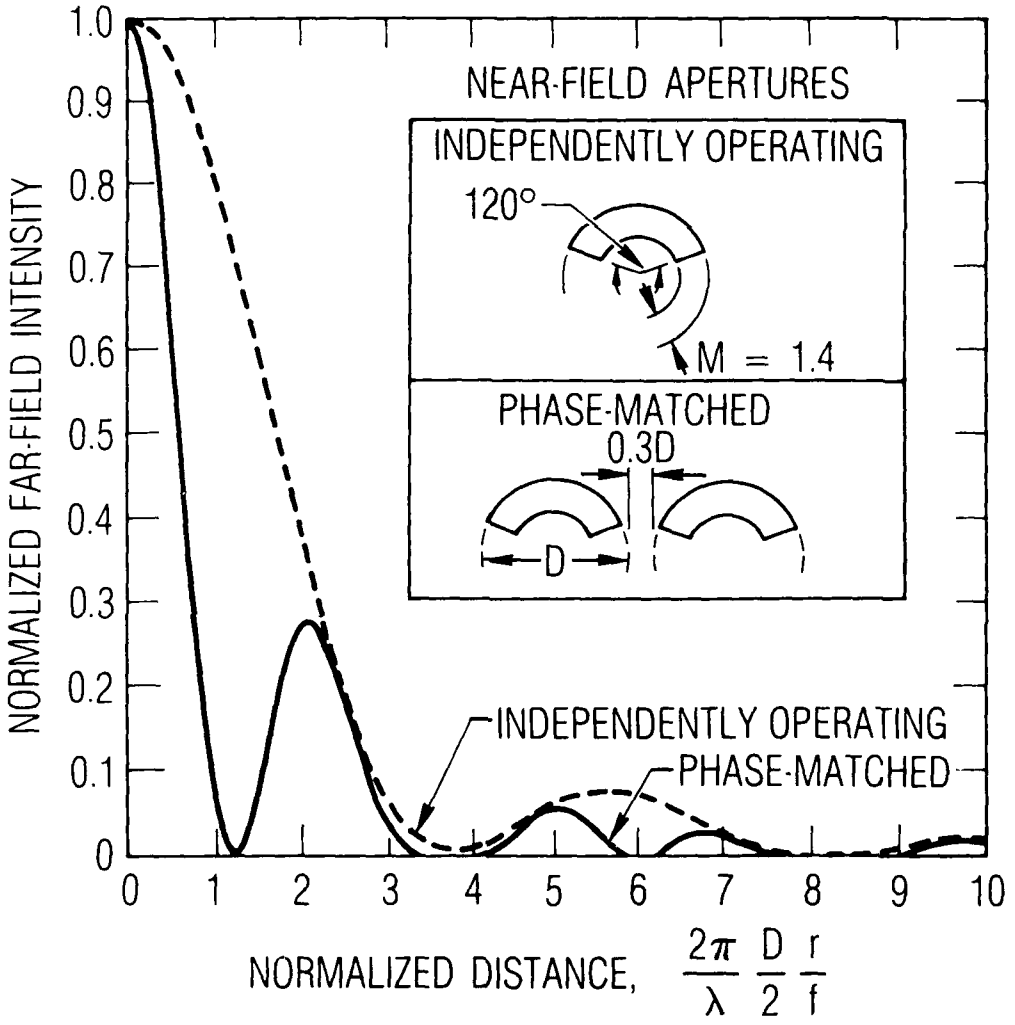

Fig. 7. Theoretical Centerline Horizontal Scans of the Far-Field Intensity Distribution for Phase-Matched and for Independently Operating Lasers

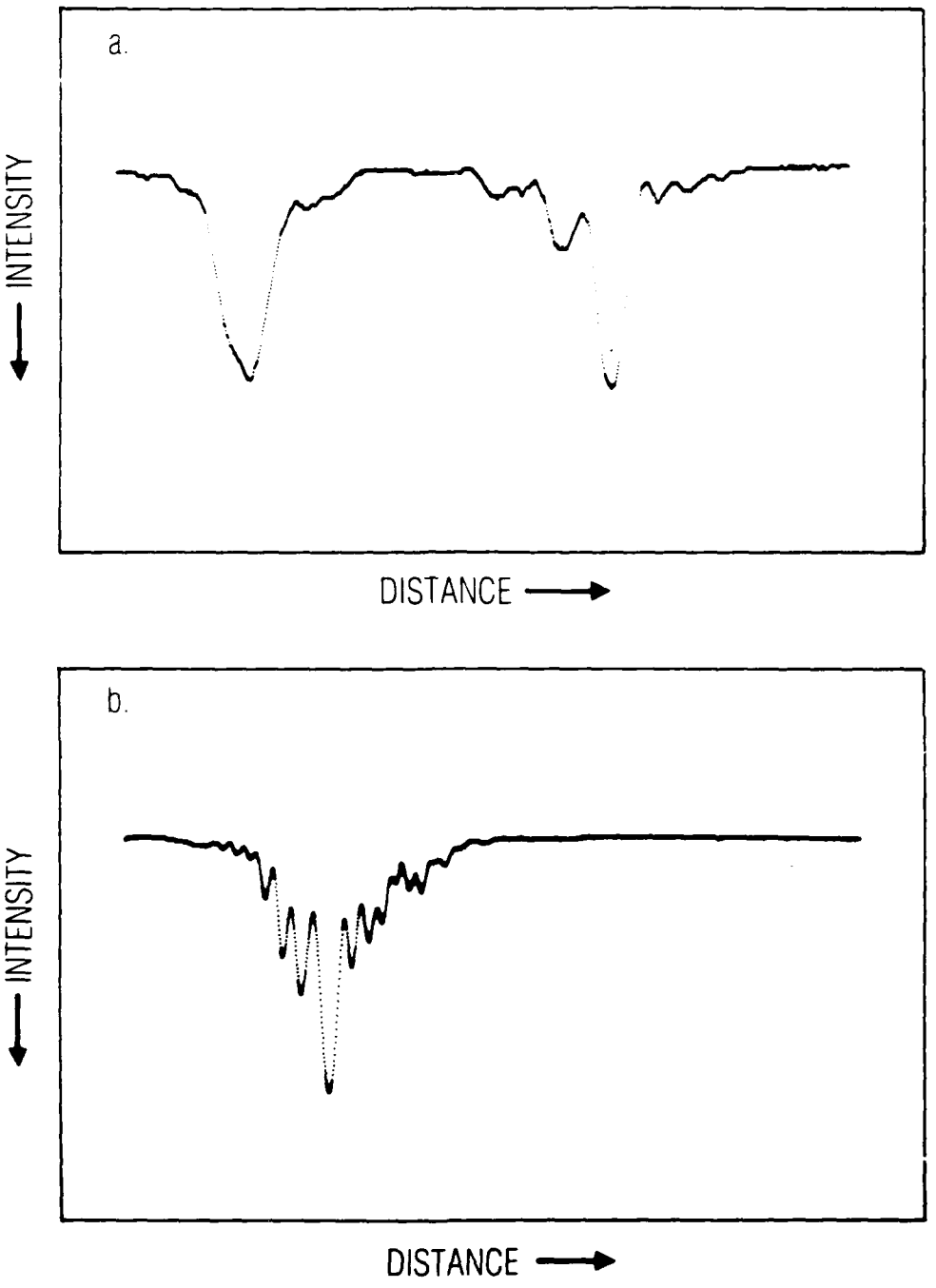

Fig. 8. (a) Far-Field Scans of the $P_2(6)$ Component of the Individual, Separated, Focused Spots of the Two Output Beams; (b) Combined Focused Spot for the Two Output Beams.

individual far-field spots of the two laser outputs, and Fig. 8b shows the single-line scan with the outputs focused to a common spot. Narrowing by a factor of 2.5 is indicated, as is the expected increase in peak intensity. This far-field measurement is extremely sensitive (on the order of a tenth-wavelength) to the external path length difference between the two beams. For a single line, this difference can be an integral number of wavelengths, while for multiline phase-matching, it must be zero. The multiline result is shown in Fig. 9, for which the narrowing is a factor of 2. This result has been degraded by a global difference in OPD as well as a possible OPD mismatch on the order of a tenth wavelength. We conclude from these far-field measurements that the expected coherent combination of the two outputs has been achieved and that small deviations from zero OPD and wave front aberrations account for our not achieving the theoretical maximum far-field intensity distribution.

It may also be noted from Figs. 8a and 9a that the beam quality of the individual beams is worse when coupled (n^2 ~1.8 in these figures) than it is uncoupled (n^2 = 1.02). We attribute this degradation to misalignment of the coupling path between the two resonators. We have observed that the near- and far-field patterns of the coupled laser outputs are sensitive to coupling path tilt. Since the coupling beams are injected converging waves, if they are tilted with respect to the resonator optic axis, they can reinforce higher order resonator modes that degrade beam quality.[7] For our experimental geometry, we estimate a 10 μrad sensitivity to tilt, and millimeter position sensitivity, for the alignment of the coupling paths to affect the coupled laser beam quality. This tilt tolerance is on the order of the accuracy and stability of the mirror mounts used, which may explain our difficulty in obtaining near diffraction-limited output from the individual coupled resonators. Note that phase-locking is much less sensitive to coupling path misalignment than is beam quality. This is analagous to the beam quality degradation that occurs in a ring resonator when the reverse wave suppressor mirror is tilted.[8] Thus the alignment sensitivity of the coupling path is roughly twice that of the individual resonators.

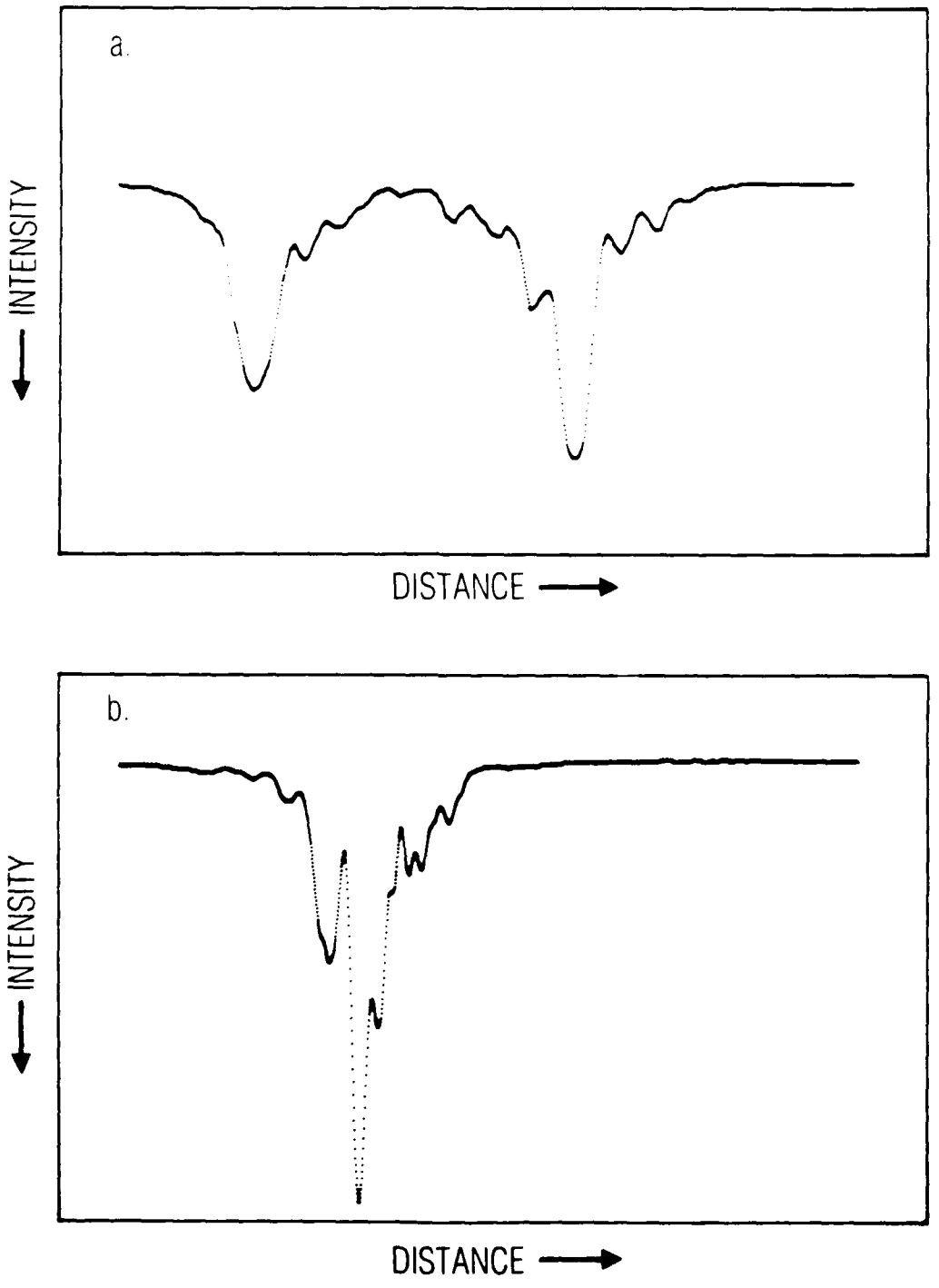

Fig. 9. (a) Far-Field Scans of the Multiline Focused Spots for the Individual, Separated Beams;(b) Far-Field Scan of the Multiline Focused Spot of the Combined Beams.

IV. CONCLUSIONS

The measurements given in this report pertain to the use of coupled lasers in a phased array. Such an array requires both phase-locking and phase-matching of the multiple outputs. Our measurements confirm that both conditions can be achieved. We have shown, with the measurements of single-line near-field fringe visibilities and mode beating, that phase-locking occurs in our strongly coupled system without resonator length sensitivity. Our multiline fringe visibility measurements and the far-field scans demonstrate that phase matching of the two outputs requires submicron length control of their external paths. Thus, phased laser array performance is most sensitive to external path length equalization, with tilt sensitivity next, while its sensitivity to wavefront aberrations is an order of magnitude less.[9]

The coupling fraction of 20% used in the present study represents strong coupling, since the injected component from one laser makes several passes through the gain region of the second laser before collapsing onto the optic axis of the second resonator, where the output mode of the resonator is established. The original 20% of the laser intensity is amplified by an order of magnitude or more on its way in and out of the second resonator. Such high intensity, injected onto the optic axis of each resonator by the other, is probably the reason that complete phase-locking occurs and that the coupled system behaves as a single laser device. We expect that as the coupling fraction is decreased, length sensitivity will increase, and ultimately independent operation of the two devices will occur.

REFERENCES

1. M. B. Spencer and W. E. Lamb, Jr., "Theory of Two Coupled Lasers," Phys. Rev. A 5, 893 (1972).

2. H. Mirels, "Performance of Two Coupled Lasers," Appl. Opt. 25, 2130 (1986).

3. H. Mirels, "Saturation Effects in Coupled Lasers with Homogenous Gain," Appl. Opt. 26, 47 (1987).

4. G. E. Palma and W. J. Fader, "Coupled Resonator Beam Combining," Proc. Soc. Photo-Opt. Instrum. Eng. 440, 153 (1983).

5. J. M. Bernard, R. A. Chodzko, and H. Mirels,"Mutual Coherence of Two Coupled Multiline Continuous-Wave HF Lasers," Opt. Lett. 12, 897 (1987).

6. D. J. Spencer, H. Mirels, and D. A. Durran, "Performance of cw HF Chemical Laser with N_2 or He Diluent," J. Appl. Phys. 43, 1151 (1972).

7. R. A. Chodzko, S. B. Mason, and E. F. Cross, "Annular Converging Wave Cavity," Appl. Opt. 15, 2137 (1976).

8. J. M. Bernard, R. A. Chodzko, and H. Mirels, "Reverse-Wave Suppressor Mirror Effects on CW HF Unstable Ring Laser Performance," Appl. Opt. 25, 666 (1986).

9. R. B. Hooker, The Effects of Aberrations in Synthetic Aperture Systems, Ph.D. Dissertation, University of Arizona (1974).

LABORATORY OPERATIONS

The Aerospace Corporation functions as an "architect-engineer" for national security projects, specializing in advanced military space systems. Providing research support, the corporation's Laboratory Operations conducts experimental and theoretical investigations that focus on the application of scientific and technical advances to such systems. Vital to the success of these investigations is the technical staff's wide-ranging expertise and its ability to stay current with new developments. This expertise is enhanced by a research program aimed at dealing with the many problems associated with rapidly evolving space systems. Contributing their capabilities to the research effort are these individual laboratories:

Aerophysics Laboratory: Launch vehicle and reentry fluid mechanics, heat transfer and flight dynamics; chemical and electric propulsion, propellant chemistry, chemical dynamics, environmental chemistry, trace detection; spacecraft structural mechanics, contamination, thermal and structural control; high temperature thermomechanics, gas kinetics and radiation; cw and pulsed chemical and excimer laser development including chemical kinetics, spectroscopy, optical resonators, beam control, atmospheric propagation, laser effects and countermeasures.

Chemistry and Physics Laboratory: Atmospheric chemical reactions, atmospheric optics, light scattering, state-specific chemical reactions and radiative signatures of missile plumes, sensor out-of-field-of-view rejection, applied laser spectroscopy, laser chemistry, laser optoelectronics, solar cell physics, battery electrochemistry, space vacuum and radiation effects on materials, lubrication and surface phenomena, thermionic emission, photosensitive materials and detectors, atomic frequency standards, and environmental chemistry.

Computer Science Laboratory: Program verification, program translation, performance-sensitive system design, distributed architectures for spaceborne computers, fault-tolerant computer systems, artificial intelligence, microelectronics applications, communication protocols, and computer security.

Electronics Research Laboratory: Microelectronics, solid-state device physics, compound semiconductors, radiation hardening; electro-optics, quantum electronics, solid-state lasers, optical propagation and communications; microwave semiconductor devices, microwave/millimeter wave measurements, diagnostics and radiometry, microwave/millimeter wave thermionic devices; atomic time and frequency standards; antennas, rf systems, electromagnetic propagation phenomena, space communication systems.

Materials Sciences Laboratory: Development of new materials: metals, alloys, ceramics, polymers and their composites, and new forms of carbon; nondestructive evaluation, component failure analysis and reliability; fracture mechanics and stress corrosion; analysis and evaluation of materials at cryogenic and elevated temperatures as well as in space and enemy-induced environments.

Space Sciences Laboratory: Magnetospheric, auroral and cosmic ray physics, wave-particle interactions, magnetospheric plasma waves; atmospheric and ionospheric physics, density and composition of the upper atmosphere, remote sensing using atmospheric radiation; solar physics, infrared astronomy, infrared signature analysis; effects of solar activity, magnetic storms and nuclear explosions on the earth's atmosphere, ionosphere and magnetosphere; effects of electromagnetic and particulate radiations on space systems; space instrumentation.